Magnification as a tool in weak lensing

Alberto Vallinotto, Scott Dodelson, and Pengjie Zhang

Phys. Rev. D **84**, 103004 — Published 14 November 2011

DOI: 10.1103/PhysRevD.84.103004

FERMILAB-PUB-10-396-T

Magnification as a Tool in Weak Lensing

Alberto Vallinotto[1], Scott Dodelson[1,2,3], Pengjie Zhang[4]
[1] *Center for Particle Astrophysics, Fermi National Accelerator Laboratory, Batavia, IL 60510*
[2] *Department of Astronomy & Astrophysics, The University of Chicago, Chicago, IL 60637*
[3] *Kavli Institute for Cosmological Physics, Chicago, IL 60637 and*
[4] *Key Laboratory for Research in Galaxies and Cosmology, Shanghai Astronomical Observatory, Nandan Road 80, Shanghai, 200030, China*

Weak lensing surveys exploit measurements of galaxy ellipticities. These measurements are subject to errors which degrade the cosmological information that can be extracted from the surveys. Here we propose a way of using the galaxy data themselves to calibrate the measurement errors. In particular, the cosmic shear field, which causes the galaxies to appear elliptical, also changes their sizes and fluxes. Information about the sizes and fluxes of the galaxies can be added to the shape information to obtain more robust information about the cosmic shear field. The net result will be tighter constraints on cosmological parameters such as those which describe dark energy.

PACS numbers:

Introduction. Weak gravitational lensing [1–3] has the potential to probe some of the most outstanding problems in cosmology. Hidden in the pattern of the ellipticities of background galaxies is information about the cosmic shear field, which in turn depends on the large scale properties of the universe, including the nature of the dark energy [4, 5]. Among the systematic hurdles that must be overcome in order to mine this information is bias in the measurements of these ellipticities. Here we focus on *multiplicative bias* [6–9], the fact that the observed ellipticity of a galaxy is related to its true ellipticity via a multiplicative factor that is not necessarily equal to one. When ellipticities are converted to convergences (where κ is the convergence along the line of sight to the background galaxies), this translates to

$$\kappa^{\rm obs}(\hat{n}, z) = b_m(z)\kappa^{\rm true}(\hat{n}, z) \qquad (1)$$

where the assumption that the multiplicative bias b_m depends only on the redshift of the background probes follows the arguments of Refs. [6–9] that the angular dependence leads only to smaller, higher-order corrections.

Here we propose a method of calibrating the multiplicative bias, exploiting the effect that weak lensing has on the sizes and fluxes of the background galaxies. While shapes are usually used to infer κ, sizes and fluxes are also distorted. As such, these observables carry information about the convergence field[1] and can also be used to improve cluster mass estimates [12]. We show here that future surveys may be able to use this information to calibrate the multiplicative bias, thereby enabling us to capture more of the information contained in the cosmic shear field. For concreteness we focus mainly on two upcoming lensing surveys: the Dark Energy Survey [13] (DES) and the Large Synoptic Survey Telescope [14] (LSST), both at a single redshift slice (so that b_m is constant).

The Impact of Lensing on Sizes and Fluxes. Weak lensing increases the size of a given galaxy by a factor of $1+\kappa$ and the flux by $1+2\kappa$, corresponding to a decrease in magnitude by $2.5\ln(1+2\kappa)/\ln(10)$. The average size and flux of galaxies in a survey, however, are affected by lensing in a more complex way due to the thresholds for inclusion in the survey. Consider Fig. 1, which depicts the size and i-magnitude distributions of galaxies observed in the Hubble-GOODS survey [15] as they might appear in DES behind a region with $\kappa = 0.1$. Cuts in size and magnitude are depicted by the vertical lines and a mean seeing of $0.9''$ has been added to the sizes. Although each individual galaxy increases in size/magnitude, the mean size/magnitude is also affected by the small/faint galaxies that are promoted into the survey by lensing. Thus, the change in the mean size/magnitude is not given by the simple relationships above.

We quantify the effect of lensing of the mean sizes and magnitudes by introducing coefficients g_s, g_m defined via

$$\begin{aligned} \langle m_i^{\rm obs}\rangle &\equiv m_0 + g_m\kappa_i^{\rm true} \qquad [\text{magnitude}] \\ \langle s_i^{\rm obs}\rangle &\equiv s_0(1+g_s\kappa_i^{\rm true}) \qquad [\text{size}]. \end{aligned} \qquad (2)$$

Here m_0 and s_0 are the mean magnitude and size in the entire galaxy sample, and the index i labels an angular pixel in which there are many galaxies, all of which are affected by the same convergence $\kappa_i^{\rm true}$. Since s_0 and m_0 are obtained by averaging over all galaxies in the survey (behind regions with both positive and negative κ), they can be determined very accurately. The mean size and magnitude of background galaxies in a pixel, therefore, contain information about the cosmic shear field affecting that pixel.

To extract this information from sizes and magnitudes, we need to know the coefficients g_m and g_s. One hint comes from the recent detection of lensing on the average flux of SDSS quasars [16]. They found a value of $g_m = -0.25$ ($-C_S$ in their notation). Using the deep HST data, we can simulate DES/LSST conditions and estimate the

[1] The distortions in size and magnitude also introduce selection bias [10, 11], which will bias cosmological results if not accounted for properly.

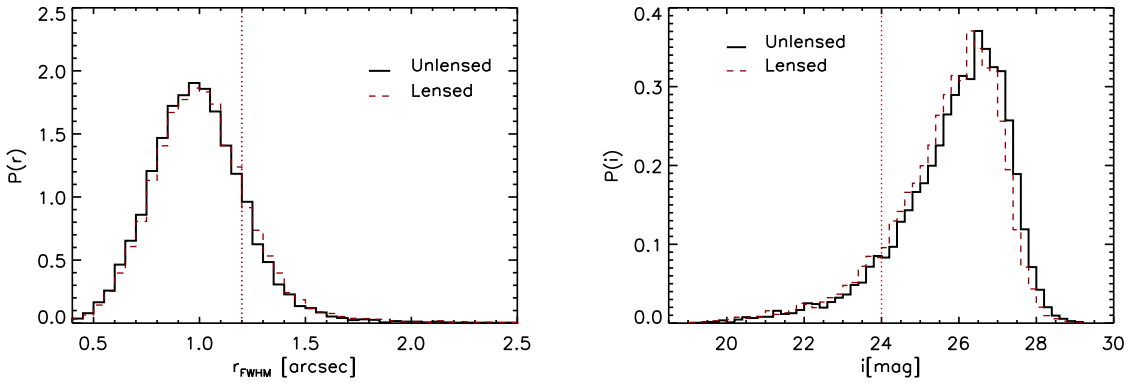

FIG. 1: Distributions of the sizes (left panel) and the magnitudes (right panel) for a DES-like survey with (dashed) and without (solid) lensing by a convergence $\kappa = 0.1$ (the specific value of κ is assumed for illustration purposes only). Regions with positive κ will therefore have larger and brighter galaxies. Vertical lines show the fiducial thresholds for the DES survey.

coefficients. We take the unlensed sizes and magnitudes, adopt a value of κ, generate a new set of simulated data by $m \to m - 2.5\ln(1+2\kappa)/\ln 10$ and $s \to s(1+\kappa)$, and then apply simulated seeing and cuts of $s^{\rm obs} > 1.2''$ and $m^{\rm obs} < 24$. The resulting means $\langle m^{\rm obs}\rangle$ and $\langle s^{\rm obs}\rangle$ then determine the g's via, e.g., $g_m = (\langle m^{\rm obs}\rangle - m_0)/\kappa$. We find $g_m = -0.3$ and $g_s = 0.25$, fairly independently of cuts and κ, so we use these values in the projections.

Estimating g_m and g_s from survey data is likely to be more difficult. The standard estimate for g_m, e.g., is

$$g_m = \left[1 - \frac{m_c N(m_c)}{\int_{-\infty}^{m_c} mN(m)dm} + \frac{N(m_c)}{\int_{-\infty}^{m_c} N(m)dm}\right]\frac{5}{\ln 10}, \quad (3)$$

where $N(m)dm$ is the number of galaxies in the magnitude interval m-$m+dm$ and m_c is the magnitude cut. This formula though neglects the real world complexities introduced by multiple cuts (size and magnitude) and the finite statistics in the magnitude bin used to estimate $N(m)$. Instead, we may need to use data from even deeper surveys to calibrate the g's for the survey of interest, just as have used used HST data here to estimate the g's for DES.

Reducing Multiplicative Bias. We now envision using all three sets of observables (ellipiticites, sizes, and magnitudes), each of which depends on $\kappa^{\rm true}$, to constrain the multiplicative bias, and therefore reduce the errors on cosmological parameters. As an illustration, we consider the case where there is only a single cosmological parameter, the amplitude of the power spectrum of the convergence, P_κ. If we had no information about the bias b_m, then ellipticity measurements alone could not determine the amplitude of the power spectrum, P_κ. Technically, if the amplitude of the power spectrum were characterized by a, with $a = 1$ being the true value, there would be a complete degeneracy between a and b_m, since

$$\begin{aligned}\langle\kappa_i^{\rm obs}\kappa_j^{\rm obs}\rangle &= b_m^2\langle\kappa_i^{\rm true}\kappa_j^{\rm true}\rangle + \delta_{ij}\sigma_\kappa^2 \\ &= a^2 b_m^2\int\frac{d^2l}{(2\pi)^2}\mathcal{P}_\kappa(l)J_0(l\theta_{ij}) + \delta_{ij}\sigma_\kappa^2 \\ &\equiv a^2 b_m^2\xi_\kappa(\theta_{ij}) + \delta_{ij}\sigma_\kappa^2 \quad (4)\end{aligned}$$

where θ_{ij} is the angular distance between the two pixels, $\mathcal{P}_\kappa$ is the (assumed known) shape of the power spectrum ($P_\kappa = a\mathcal{P}_\kappa$), and σ_κ is the rms of the ellipticities in the absence of a signal, due to shape noise and measurement errors. Observations of ellipticities then depend only on the product ab_m, so there is a complete degeneracy between these two parameters.

The sizes and magnitudes contain information that break this degeneracy. A simple way to exploit this information is to consider the full set of two-point functions of (convergence, size, and magnitude) for each pair of pixels:

$$\begin{aligned}\langle\kappa_i^{\rm obs}(s_j^{\rm obs} - s_0)\rangle &= a^2 b_m g_s s_0\xi_\kappa(\theta_{ij}), \quad (5)\\ \langle\kappa_i^{\rm obs}(m_j^{\rm obs} - m_0)\rangle &= a^2 b_m g_m\xi_\kappa(\theta_{ij}), \quad (6)\\ \langle(s_i^{\rm obs} - s_0)(s_j^{\rm obs} - s_0)\rangle &= \delta_{ij}\sigma_s^2\left[1 + a^2 g_s^2\xi_\kappa(\theta=0)\right] \\ &\quad + a^2 g_s^2 s_0^2\xi_\kappa(\theta_{ij}), \quad (7)\\ \langle(s_i^{\rm obs} - s_0)(m_j^{\rm obs} - m_0)\rangle &= \delta_{ij}\sigma_{ms}^2 \\ &\quad + a^2 g_m g_s s_0\xi_\kappa(\theta_{ij}), \quad (8)\\ \langle(m_i^{\rm obs} - m_0)(m_j^{\rm obs} - m_0)\rangle &= \delta_{ij}\sigma_m^2 + a^2 g_m^2\xi_\kappa(\theta_{ij}). \quad (9)\end{aligned}$$

The variances σ_s^2 and σ_m^2 include contributions from intrinsic scatter in sizes and magnitudes and also the measurement errors expected in the survey, while σ_{ms}^2 denotes the (intrinsic) covariance between the sizes and fluxes.

The data set will then contain $3N$ numbers: the average size, magnitude, and shear/convergence of all galaxies in a set of N pixels. To assess how powerful this

Probe	Mean	Dispersion	g	Cut
Size (arcsec)	1.5 (0.9)	0.33 (0.266)	0.25	1.2 (0.7)
Magnitude	22.7 (24.4)	1.1 (1.26)	-0.3	24 (26)

TABLE I: Assumed values for sizes and magnitudes of DES and LSST. Values for the sizes and magnitudes of *single* galaxies for the DES survey, so the scatter in a single pixel containing $M = 15$ galaxies is $\sigma_s = 0.33''/\sqrt{15}$ and $\sigma_m = 1.1/\sqrt{15}$. Values in parentheses are those adopted for LSST, with $M = 100$ assumed. The correlation coefficient used throughout is $\rho_{ms} = -0.46$.

information will be, we construct the Fisher matrix. The 2×2 Fisher matrix is

$$F_{\alpha\beta} = \frac{1}{2}\mathrm{Tr}\left[C_{,\alpha}C^{-1}C_{,\beta}C^{-1}\right]. \qquad (10)$$

where α, β run over the two parameters a and b_m, the trace is over all the $3N$ observables and C is their $3N \times 3N$ covariance matrix with elements given in Eqs. (4-9).

DES (LSST) will cover about $5,000\,(20,000)$ sq. degrees, and we consider pixels of size $\Delta\theta^2 = 10$ square arcmin. The total number of pixels is then $= 1.8 \times 10^6\,(7.2 \times 10^6)$. We focus only on the redshift range $z \in [0.9, 1.1]$ with an expected number of galaxies per pixel of $M = 15\,(100)$. Furthermore, we assume that galaxies' sizes and magnitudes within each pixel are statistically independent[2] and we neglect the fact that, because of clustering, the galaxies appearing in a single pixel may be systematically closer or further from the observer than the mean redshift. The parameters assumed for magnitudes and sizes are summarized in Tab. I.

Fig. 2 shows the projected constraints from DES assuming that all the pixels are uncorrelated (so the Fisher matrix is simply the one-pixel Fisher matrix times 1.8×10^6). The figure shows that multiplicative bias in a single redshift bin can be pinned down at the 5% level with the aid of size and magnitude measurements. Also shown is the projection for LSST. Here the requirements on the bias will be more severe because the statistical power is much higher [9], and indeed the extra information does pin down multiplicative bias at the percent level.

The projected errors in Fig. 2 retain the degeneracy between a and b_m that afflicts the shear-only measurements. This is an indication that the shear measurements carry the most statistical weight. To confirm this, consider the signal to noise of the shear measurement. Taking the ratio of the two terms on the right in Eq. (4) and weighting by the number of galaxies M

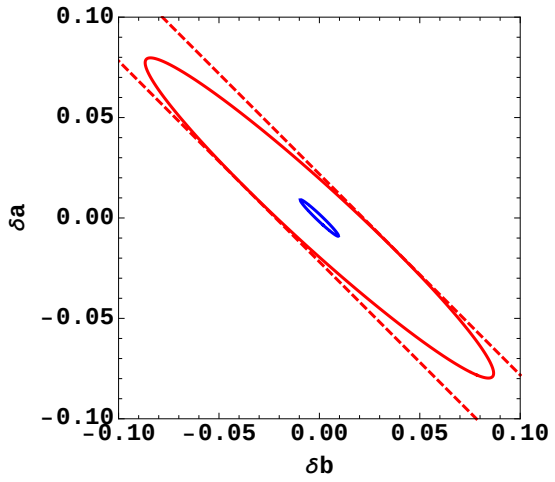

FIG. 2: Projected constraints on the multiplicative bias b_m and amplitude of the power spectrum a for two surveys obtained by including information on sizes and magnitudes. The red solid contour shows the projection for DES (5000 square degrees) with 1.5 galaxies per square arcminute in the redshift range [0.9, 1.1]. The red dashed contour shows the corresponding (degenerate) region for DES in the case that information from sizes and magnitudes were *not* included in the analysis. The blue solid contour shows projections for an LSST-like survey with 10 galaxies per square arcminute in this redshift range and 20,000 square degrees.

in a pixel leads to $(S/N)_{\rm shear} \simeq \sqrt{M\xi/\sigma_\kappa^2}$. For DES (LSST) this is of order 0.1 (0.3). By contrast, a similar estimate for the size measurement using Eq. (7) leads to $(S/N)_{\rm size} \simeq \sqrt{M g_s^2 s_0^2 \xi/\sigma_s^2}$, or 0.04 (0.07) for DES (LSST). Although the dispersion in sizes is comparable to shape noise, the signal is suppressed by a factor of g_s. A similar estimate for the magnitudes yields even smaller signals. So the shear measurements dominate the constraints, and the utility of the size/magnitude measurements is to break the degeneracy between the amplitude of the clustering (a) and the multiplicative bias (b_m).

We have neglected correlations between pixels. When these are added in, the constraints will become tighter. We have not computed the Fisher matrix including all correlations, but we have studied how the constraints with and without correlations compare for smaller fields as the number of pixels increases . These studies suggest that there is additional information in the correlations which will further tighten the constraints on multiplicative bias by at least 10%.

Conclusions. Weak lensing affects several observed properties of galaxies: not only does it distort their shapes, but it also alters their observed sizes and magnitudes. We have demonstrated that these other distortions can turned into an asset: the lensing effect on the average galaxy size and magnitude helps to constrain multiplicative bias. The comprehensive way to determine how successful these new observables will be at improving cosmological constraints is to add them to the program

[2] A heuristic justification of this assumption relates to the fact that the bias is roughly constant for objects with mass smaller than clusters. It then follows that the probabilities of finding a $10^{11}\ M_\odot$ or a $10^{12}\ M_\odot$ galaxy near a $10^{11}\ M_\odot$ should be roughly equal.

initiated by Bernstein [17], where the Fisher matrix for all parameters (cosmological and nuisance) is determined for a fixed set of measurements of κ and the density of sources. Here we have estimated the improvement in a simple setting where only the amplitude of the power spectrum is unknown. This simple example suggests that the added information is potentially useful and should be incorporated into the more comprehensive program and ultimately into the full analysis pipeline of upcoming surveys.

Acknowledgments. We thank Eduardo Rozo and Fabian Schmidt for useful comments and discussions. This work has been supported by the US Department of Energy, including grant DE-FG02-95ER40896, and by National Science Foundation Grant AST-0908072. PJZ acknowledges the support of the one-hundred talents program of the Chinese Academy of Sciences (CAS), the national science foundation of China (grant No. 10821302 & 10973027), the CAS/SAFEA International Partnership Program for Creative Research Teams and the 973 program (grant No. 2007CB815401). AV is supported by the DOE at Fermilab. AV thanks the Fermilab Center for Particle Astrophysics for hospitality during the final stages of this work.

[1] M. Bartelmann and P. Schneider, Phys. Rept. **340**, 291 (2001), astro-ph/9912508.
[2] P. Schneider (2005), astro-ph/0509252.
[3] D. Munshi, P. Valageas, L. Van Waerbeke, and A. Heavens, Phys. Rept. **462**, 67 (2008), astro-ph/0612667.
[4] R. R. Caldwell and M. Kamionkowski, Ann. Rev. Nucl. Part. Sci. **59**, 397 (2009), 0903.0866.
[5] J. Frieman, M. Turner, and D. Huterer, Ann. Rev. Astron. Astrophys. **46**, 385 (2008), 0803.0982.
[6] D. Huterer, M. Takada, G. Bernstein, and B. Jain, Mon. Not. Roy. Astron. Soc. **366**, 101 (2006), astro-ph/0506030.
[7] C. Heymans et al., Mon. Not. Roy. Astron. Soc. **368**, 1323 (2006), astro-ph/0506112.
[8] R. Massey et al., Mon. Not. Roy. Astron. Soc. **376**, 13 (2007), astro-ph/0608643.
[9] A. Amara and A. Refregier, Mon. Not. Roy. Astron. Soc. **391**, 228 (2008), 0710.5171.
[10] F. Schmidt, E. Rozo, S. Dodelson, L. Hui, and E. Sheldon, Phys. Rev. Lett. **103**, 051301 (2009), 0904.4702.
[11] F. Schmidt, E. Rozo, S. Dodelson, L. Hui, and E. Sheldon, Astrophys. J. **702**, 593 (2009), 0904.4703.
[12] E. Rozo and F. Schmidt (2010).
[13] T. Abbott et al. (Dark Energy Survey) (2005), astro-ph/0510346.
[14] Z. Ivezic et al. (2008), 0805.2366.
[15] M. Giavalisco et al. (GOODS), Astrophys. J. **600**, L93 (2004), astro-ph/0309105.
[16] B. Menard, R. Scranton, M. Fukugita, and G. Richards (2009), 0902.4240.
[17] G. M. Bernstein, Astrophys. J. **695**, 652 (2009), 0808.3400.